JAERI-M
86-161

IMPURITY TRANSPORT IN OHMICALLY HEATED JT-60 PLASMA

October 1986

Toshio HIRAYAMA, Tatsuo SUGIE, Akira SAKASAI
Hirotaka KUBO, Yoshihiko KOIDE, Nobuo AKAOKA
Hiroshi TAKEUCHI and Masayuki NAGAMI

日本原子力研究所
Japan Atomic Energy Research Institute

JAERI-M レポートは，日本原子力研究所が不定期に公刊している研究報告書です。
入手の問合わせは，日本原子力研究所技術情報部情報資料課（〒319－11 茨城県那珂郡東海村）あて，お申しこしください。なお，このほかに財団法人原子力弘済会資料センター（〒319-11 茨城県那珂郡東海村日本原子力研究所内）で複写による実費頒布をおこなっております。

JAERI-M reports are issued irregularly.
Inquiries about availability of the reports should be addressed to Information Division, Department of Technical Information, Japan Atomic Energy Research Institute, Tokai-mura, Naka-gun, Ibaraki-ken 319-11, Japan.

編集兼発行　日本原子力研究所
印　　刷　山田軽印刷所

JAERI-M 86-161

IMPURITY TRANSPORT IN OHMICALLY HEATED JT-60 PLASMA

Toshio HIRAYAMA, Tatsuo SUGIE, Akira SAKASAI,
Hirotaka KUBO, Yoshihiko KOIDE, Nobuo AKAOKA,
Hiroshi TAKEUCHI and Masayuki NAGAMI

Department of Large Tokamak Research
Naka Fusion Research Establishment
Japan Atomic Energy Research Institute
Naka-machi, Naka-gun, Ibaraki-ken

(Received October 11, 1986)

In the Ohmically heated plasma of JT-60, the transport of impurities has been studied by VUV and soft X-ray crystal spectroscopies, and from bolometer and soft X-ray diode signals, along with one-dimensional impurity transport code. Changing over a discharge from the limiter mode to the divertor mode, the decay of the bolometer signals was measured and the time constant was about 0.3 sec in the central chord. Temporal evolutions of T_i *XIII*(23.356Å), T_i *XX*(259.3Å) and T_i *XXI* (resonance line) were obtained in two different discharges with I_p=2*MA* which a piece of titanium was accidentally injected into. The comparison of the time behaviour of the respective lines with the simulation results by a diffusive/convective transport model shows that the anomalous diffusion coefficient is about 1.0 m^2/s and convective inward velocity is not seen.

Keywords: Tokamak, Impurity Transport, Ohmically Heated Plasma, JT-60

オーミック加熱時のＪＴ－60プラズマにおける不純物輸送

日本原子力研究所那珂研究所臨界プラズマ研究部
平山　俊雄・杉江　達夫・逆井　　章
久保　博孝・小出　芳彦・赤岡　伸雄
竹内　　浩・永見　正幸

（1986年10月11日受理）

ＪＴ－60のオーミック加熱時のプラズマについて，不純物輸送の特性を，ＶＵＶ分光器，軟Ｘ線領域結晶分光器，ボロメータ，及び軟Ｘ線ダイオード検出器による計測と，一次元不純物輸送コードを用いて解析した。プラズマ放電をリミタからダイバータに切り換えることにより，不純物の放射損失の減衰曲線を測定し，0.34秒の時定数を得た。ダイバータ放電中に落下したチンタ不純物の線強度（TiXIII，23.356Å，TiXX，259.3Å，TiXXI）の時間変化を，拡散／移流輸送モデルの計算結果と比較することにより，拡散係数として1m²/s，移流速度無しの時実験結果と良い一致を得た。

Contents

目　　次

1. Introduction

Impurity problem is one of the serious factors which should affect the tokamak plasma, following the degradation of confinement properties. Therefore, impurity transport phenomena have been paid attention in the last few years. In Ohmically heated PDX discharges [1], time- and space-resolved measurements of He^{++} density following a short puff of helium gas into the plasma edge are fitted with use of a diffusive/convective transport model with diffusion coefficient of $D_A=(2.1\pm0.9)\ m^2/s$ and convective inward velocity $v(r)=(0.8\pm0.3)D_A\partial(\ln n_e)/\partial r$. Decay time of the line emissivity of titanium injected into neutral beam heated Doublet III discharges by a laser blow-off technique is simulated with a diffusive transport model including the neoclassical impurity particle flux and the $D_A(r)$ of $(4\text{-}5)\times10^{19}/n_e(r)\ m^2/s$ is obtained as an anomalous diffusion coefficient, for discharges from the L-mode (bad confinement) to the H-mode (good confinement) with a modest beam power (<3-4 MW) [2]. Contrary to a discharge forcefully heated with a beam power of ~7.5MW [3], the modest heating results in the H-mode plasma with H_α burst in which impurity radiation loss does not accumulate into the discharge and the clear dependence of impurity transport properties is improved particle confinement time only proportional to the increment of the electron density, as a consequence of an improved confinement properties. On the other hand, in a neutral beam heated ASDEX plasma [4], H-mode discharges of H_α burst-free are obtained and then, strong impurity accumulation in the center of the discharge is observed. This accumulation often leads to excessive radiation loss and results in a thermal collapse of the good confined plasma. The degree of central impurity accumulation is found to be strongly dependent of the charge of the impurity ion in the central core of

PBX H-mode discharge [5]. Assuming a diffusive/convective transport model, reasonable fits to time-evolving redistribution of impurities, in the plasma associated with large sawteeth are obtained with the diffusion coefficient of D_A=0.1 m^2/s, and a dimensionless peaking parameter of C_V=4 ($C_V=av/2D_A$, where a is the minor radius) for light impurities and C_V=20 for metal impurities. They conclude that transport inside the q=1 surface appeares to be close to neoclassical. In TFR [6], transport of impurities in Ohmic and ICRF-heated plasmas is studied by laser blow-off injection of vanadium. The best agreement between the experimental and simulated radiances of central ions is obtained for D_A=0.4 m^2/s and C_V=3. No difference is found between the two experimental situations although degradation of the energy confinement time is observed in an ICRF-heated plasma. Additionally, it is declared that the impurity transport parameters are not modified by the internal disruption. Recently, in JET, impurity transport is studied by utilizing a piece of iron fallen into a discharge and D_A is estimated to be of 0.6 m^2/s within the framework of a purely diffusive transport model [7]. It may be generally said that for the impurity transport properties in a tokamak plasma from medium size machines to large ones, the diffusion coefficient is (0.4-2.0) m^2/s and the peaking factor is (1-3), excepting the parameters in PBX H-mode plasma. The existence of convective inward velocity strongly modifies the plasma confinement properties, especially of beam heated plasma so as to be seen in ASDEX and PBX. Therefore, it is important to clarify the impurity transport properties in large tokamaks attaining the break-even condition.

JT-60 is a unique device with a poloidal divertor in three large tokamaks. Therefore, we can aggressively make the impurity control experiment due to changing over a discharge mode from limiter to divertor or vice versa. We also study impurity transport for some discharges into which a piece of titanium was

accidentally injected.

In this paper, section 2 presents bolometric results obtained by changing over a discharge from the limiter operation to the divertor operation, and VUV line radiances of titanium and crystal spetroscopic results observed in particular discharges. After a short description of a diffusive/convective transport model in section 3, we will, in section 4, deal with transport properties by fitting the time evolution of individual spectral lines with the transport model. The summary and discussion are given in section 5.

2. Experimental Results

In order to study the divertor effect on the impurity confinement, the magnetic configuration was changed from the limiter mode to the divertor one during the flat-top phase of hydrogen discharge (shot number of E552) with plasma current I_P = 0.5 MA and toroidal magnetic field B_t = 3.0 T. Major and minor radii were 3.05 m and 0.9 m in the limiter mode and 3.15 m and 0.83 m in the divertor mode, respectively. Figure 1 shows the typical evolution of the radiation power along the central chord from the bolometric measurement [8]. During the change of the discharge mode, the electron density was kept almost constant. It is clearly seen that the radiation loss rapidly decreased to one third of it, following the divertor mode. The decay time accounts to 0.34 sec for the central chord. If there were no recycling of impurity particles, the decay time of radiation power could have represented the impurity particle confinement time. The temporal evolution of the radiation power is affected by both processis of transport and recycling. The recycling, lower ionized

accidentally injected.

In this paper, section 2 presents bolometric results obtained by changing over a discharge from the limiter operation to the divertor operation, and VUV line radiances of titanium and crystal spetroscopic results observed in particular discharges. After a short description of a diffusive/convective transport model in section 3, we will, in section 4, deal with transport properties by fitting the time evolution of individual spectral lines with the transport model. The summary and discussion are given in section 5.

2. Experimental Results

In order to study the divertor effect on the impurity confinement, the magnetic configuration was changed from the limiter mode to the divertor one during the flat-top phase of hydrogen discharge (shot number of E552) with plasma current I_P = 0.5 MA and toroidal magnetic field B_t = 3.0 T. Major and minor radii were 3.05 m and 0.9 m in the limiter mode and 3.15 m and 0.83 m in the divertor mode, respectively. Figure 1 shows the typical evolution of the radiation power along the central chord from the bolometric measurement [8]. During the change of the discharge mode, the electron density was kept almost constant. It is clearly seen that the radiation loss rapidly decreased to one third of it, following the divertor mode. The decay time accounts to 0.34 sec for the central chord. If there were no recycling of impurity particles, the decay time of radiation power could have represented the impurity particle confinement time. The temporal evolution of the radiation power is affected by both processis of transport and recycling. The recycling, lower ionized

impurity ions enhance the radiation power at the plasma boundary by a factor of 10 and result in making apparent decay time enlarged. Therefore, the decay time observed is apparently longer than the particle confinement time.

There are two discharges in which the spectral line intensities of titanium suddenly increase and subsequently decrease ; I_p = 2.0 MA, B_t = 4.5 T and hydrogen diverted plasma. During the flat top of discharge, line radiation is detected in the 0.5-50 nm VUV region by two units of flat field grazing-incident spectrometers with 512 and 1024 channel detectors. Figure 2 shows the temporal evolution of plasma current in the discharge of E1605 and the electron density profiles after accidental injection of a piece of titanium. Figure 3 shows the temporal evolution of chordal electron densities and the central electron temperature and the arrow shows the injection time. The soft X-ray, in fig. 4, are detected by fifteen channel pin diode arrays with B_e foil filter providing low energy cut-off at 4.5 KeV. Although the rapid increase of loop voltage appears at the injection time, the central electron temperature keeps to be almost constant. In the decaying stage of soft X-ray diode signals, the electron density begins to decrease owing to cut of fuelling gas. The change of the electron density, however, remains slight through our interesting time. In another shot of E1968, the temporal evolution of the He-like Ti^{20+} ion resonance line is detected in a current rump up phase by a crystal spectrometer (silicon plate, crystal cut 224) of the Johann type. The temporal evolutions of plasma current and of the electron density profile after the injection are shown in fig. 5, with the arrow corresponding to the injection time.

The electron temperature profile is usually obtained by six channel Thomson scattering measurements and the time evolution of the central electron

temperature by second-harmonic electron cyclotron emission with the time resolution of 15 ms. The electron density profile is deduced from fitting chordal integral values, which is calculated with an assumed parabolic type profile function on the magnetic flux surface from a magnetic equilibrium code [9], to the values of three channel submilimeter interferometer. Another density profile is also obtained from the Thomson scattering data of which absolute value is normalized to the value of the submilimeter at the central chord, and gives good agreement with the profile from the submilimeter. Figure 6-a shows the magnetic flux surface at 6.5 sec in the discharge of E1605, in which a piece of titanium is accidentally injected at ~ 6.3 sec. Figure 6-b shows agreement between the measurements from the submilimeter interferometer and the chordally integrated profile of fitted function. Taking into account the shift of magnetic flux surface, the profile of the electron density is reduced to the one-dimensional profiles as shown in fig.6-c.

3. Transport Models

A one dimensional time-dependent, multi-species impurity code, which is incorporated in the tokamak code system of LIBRARY [10], is employed to calculate the impurity ion density profiles and the line radiation respective to the titanium lines. The time evolution of the density is expressed as

$$\frac{\partial n_k}{\partial t} = -\frac{1}{r}\frac{\partial}{\partial r}(r\Gamma_k) + S_k - \frac{n_k}{\tau_{\parallel}} \qquad (1)$$

where n_k is the density of k-th charge state ion, Γ_k is the particle flux, S_k is the source term, and $n_k/\tau_{\parallel}$ is the loss term along the magnetic lines in the

temperature by second-harmonic electron cyclotron emission with the time resolution of 15 ms. The electron density profile is deduced from fitting chordal integral values, which is calculated with an assumed parabolic type profile function on the magnetic flux surface from a magnetic equilibrium code [9], to the values of three channel submilimeter interferometer. Another density profile is also obtained from the Thomson scattering data of which absolute value is normalized to the value of the submilimeter at the central chord, and gives good agreement with the profile from the submilimeter. Figure 6-a shows the magnetic flux surface at 6.5 sec in the discharge of E1605, in which a piece of titanium is accidentally injected at ~ 6.3 sec. Figure 6-b shows agreement between the measurements from the submilimeter interferometer and the chordally integrated profile of fitted function. Taking into account the shift of magnetic flux surface, the profile of the electron density is reduced to the one-dimensional profiles as shown in fig.6-c.

3. Transport Models

A one dimensional time-dependent, multi-species impurity code, which is incorporated in the tokamak code system of LIBRARY [10], is employed to calculate the impurity ion density profiles and the line radiation respective to the titanium lines. The time evolution of the density is expressed as

$$\frac{\partial n_k}{\partial t} = -\frac{1}{r}\frac{\partial}{\partial r}(r\Gamma_k) + S_k - \frac{n_k}{\tau_\parallel} \qquad (1)$$

where n_k is the density of k-th charge state ion, Γ_k is the particle flux, S_k is the source term, and $n_k/\tau_\parallel$ is the loss term along the magnetic lines in the

scrape-off region. Based on a diffusive/convective transport model, the particle flux Γ_k for the k-th charge state ion is given by

$$\Gamma_k(r) = -D_A(r)\frac{\partial n_k}{\partial r} + V_A(r) n_k \tag{2}$$

where $D_A(r)$ is the radial diffusion coefficient and $V_A(r)$ is a convective velocity. Connecting with a shape parameter, a convective velocity is written as $V_A(r) = -C_V D_A 2r/a^2$. The diffusion coefficient is assumed to be radially constant.

In the plasma periphery (r>a), a limiter scrape-off model is employed. The cross field diffusion in this region is assumed to be the Bohm diffusion D_B, and V_A=0. The particles are lost along the field lines to the limiter with an averaged flow velocity $V_f = C_f\sqrt{T_e/m_i}$, where m_i is the background ion mass and T_e is the electron temperature. In the following simulation, we choose C_f=1. Thus, a parallel loss time is given as $\tau_\parallel = \pi qR/V_f$. Although we do not have the measurement of the boundary plasma, we apply the general feature in the scrape-off layer plasma as

$$n_e(r) = n_e(a)\exp\left(-\frac{r-a}{\lambda_n}\right) \tag{3}$$

$$T_e(r) = T_e(a)\exp\left(-\frac{r-a}{\lambda_T}\right) \tag{4}$$

where λ_n and λ_T are the fall-off lengths of the electron density and the electron temperature. Using $T_e(a)$= 50 eV, the density fall-off length $\sqrt{\tau_\parallel D_B}$ is about 1.5 cm and the electron temperature fall-off length [11] is about 0.6 cm. The width of a scrape-off layer is taken to be 4 cm.

The source term is given as

$$S_k = n_e\alpha_{k-1}n_{k-1} - (n_e\alpha_k + n_e\beta_k)n_k + n_e\beta_{k+1}n_{k+1} \tag{5}$$

where α_k and β_k are ionization and recombination rates, respectively, calculated by Hulse's multi ion model [12] . The line radiances respective to the measurements are calculated using the multi ion model and are deduced to the averaged line emission for the specified charge state ion. Impurity neutral density profile is calculated from the Boltzmann equation in a cylindrical geometry, with the assumption of the neutral energy of 2 eV.

4. Numerical simulation of titanium emission

In order to interpret spectroscopic data by using the one-dimensional impurity transport code, the deduced one-dimensional profile of electron density is employed in time. On the other hand, we have to assume an electron temperature profile except the central value, because of unexpected injection time. Therefore, we estimate the electron temperature profile from the one in different discharges on the same conditions. The results are not so sensitive to uncertainty of temperature profile except for low charge state ions, within this work.

The incoming neutral particle flux as an accidental titanium injection is applied so that the content of titanium ion in the plasma may become 0.1 %, which is roughly estimated from the increment of the electron density, with a delay time of 5 ms. The maximal content for the case of no inward convection, however, results in 0.02 % due to assumed zero recycling rate and to the time constant of 1 ms for the impurity content control.

where α_k and β_k are ionization and recombination rates, respectively, calculated by Hulse's multi ion model [12]. The line radiances respective to the measurements are calculated using the multi ion model and are deduced to the averaged line emission for the specified charge state ion. Impurity neutral density profile is calculated from the Boltzmann equation in a cylindrical geometry, with the assumption of the neutral energy of 2 eV.

4. Numerical simulation of titanium emission

In order to interpret spectroscopic data by using the one-dimensional impurity transport code, the deduced one-dimensional profile of electron density is employed in time. On the other hand, we have to assume an electron temperature profile except the central value, because of unexpected injection time. Therefore, we estimate the electron temperature profile from the one in different discharges on the same conditions. The results are not so sensitive to uncertainty of temperature profile except for low charge state ions, within this work.

The incoming neutral particle flux as an accidental titanium injection is applied so that the content of titanium ion in the plasma may become 0.1 %, which is roughly estimated from the increment of the electron density, with a delay time of 5 ms. The maximal content for the case of no inward convection, however, results in 0.02 % due to assumed zero recycling rate and to the time constant of 1 ms for the impurity content control.

Figure 7-a shows the comparison of experimental peripheral line radiance (T_i *XIII* 23.256Å) with simulated one for D_A=1.0m^2/s and C_V=0. This comparison is almost independent of the transport parameters, because of the passing ion in the ionization dominant process. The temporal evolution of this low ionized ion radiance, however, corresponds to the one of incoming ion flux. The agreement between time behaviours of peripheral line radiance shows that an assumed incoming neutral-particle flux would appear quite reasonable.

The time resolved measurement of T_i *XX* (259.3Å), which has a peak radiance nearly $r\sim a/2$ for plasma parameters with $T_e(0)\sim 2.2KeV$, is fitted with the diffusive/convective transport model and agrees with simulated one for D_A=1.0m^2/s and C_V=0, as shown in fig. 7-b. Since the temperature modulation due to the sawtooth, of which inversion radius is about $a/4\sim a/3$ at the discharge of 2 MA, has little effect on the radiance of this ion, the electron temperature profile is assumed to be constant in time and the effect of the sawtooth on the impurity transport is not included.

A similar comparison is performed for the line radiance of central ion (T_i *XXI* resonance line) observed in another shot of E1968. Figure 8 shows the experimental and simulated radiances of central ion and the best fitness is again found for D_A=1.0m^2/s and C_V=0. The increment of this line happens to be observed at a current rump up phase when there is no sawtooth oscillation. Therefore, the sawtooth effect is not included in this simulation, too.

Figure 9 shows the comparison between the profile of soft X-ray diode array signals and the simulated one for the shot of E1605. The transport parameters of D_A=1.0m^2/s and C_V=0 well reproduce the temporal evolution of the profile during a decaying stage.

5. Summary and Discussion

Even in two different discharges, the time constant of the line radiances by the accidental titanium injection is 180 ms for T_i *XX* line and 160 ms for T_i *XXI* line, respectively. It is quite attractive that the time constant value of the central peaked ion of T_i *XXI* is almost same as the one of T_i *XX* ion peaked at $\sim a/2$. That no convective inward flow velocity exits should be responsible for the concurrence of the time constant, resulting in the broad profile of T_i^{19+} ion. Really, observed same decay time in the different ionization stages is consistent with the transport analysis $C_V=0$ and $D_A=1.0m^2/s$ which is the same order as Doublet III scaling of $4\times10^{19}/n_e$ for $n_e\sim3\times10^{19}$. Whereas the value of the anomalous diffusion coefficient is not so different from the values estimated in many other tokamaks, the characteristic of no convective inward flow is a quite distinguished feature of JT-60 plasma.

In transport steady state, no impurity ion flux ($\Gamma_k=0$) exists in the core plasma, which is a source/sink free region. Therefore, from eq. (2), a convective velocity is given in terms of the total impurity density as $n_z=\Sigma n_k$,

$$\frac{V_A(r)}{D_A} = \frac{\partial \ln n_z}{\partial r}. \tag{6}$$

According to the neoclassical impurity transport, the impurity density profile is connected with the hydrogenic ion density profile in steady state, as $n_z(r)\propto n_i(r)^Z$, where Z is the ionic charge state number and n_i the hydrogenic ion density. The n_z may be related to the electron density profile via $n_z(r)\propto n_e(r)^{C_v}$, which will be similar to the relation based on the neoclassical impurity transport. The convective velocity term of eq. (6) can be recast with above assumed relation into the form [1]

$$\frac{V_A(r)}{D_A} = C_V \frac{\partial \ln n_e(r)}{\partial r}. \qquad (7)$$

If this relation is hold so as to be successfully seen in PDX, the flat electron density profile observed in JT-60 [13] will suggest a weak convective inward flow.

Figure 10 shows the dependence of the temporal evolution of titanium ion density profiles on the transport parameters. Apart from the absolute value of each ionized charge state ion, the presence of a convective inward velocity ($C_V = 1$) brings no remarkable difference in the shape of profiles of total ion density and Ti^{20+} ion density, which takes the main part of the soft X-ray signals. Therefore, it would be very difficult to distinguish the difference in impurity transport from spatial profile of impurity ions due to the spectroscopic measurements. Impurity tracer experiment will become more important, because a slight difference in impurity transport appears in the time evolution. Impurity study using a tracer like as laser blow-off injection experiment has been carried out by utilizing a change of impurity level at an instantaneous limiter discharge during a divertor one. A more detailed transport analysis of those measurements will be reported later.

Acknowledgement

The authors wish to thank the members of JT-60 team who have contributed to the JT-60 project throughout its progress. Especially, we wish to express our appreciation to Dr. T. Fukuda for the submilimeter measurement, to Dr. M. Sato for the ECE measurement, to Dr. H. Yoshida for the Thomson scattering

$$\frac{V_A(r)}{D_A} = C_V \frac{\partial \ln n_e(r)}{\partial r}. \qquad (7)$$

If this relation is hold so as to be successfully seen in PDX, the flat electron density profile observed in JT-60 [13] will suggest a weak convective inward flow.

Figure 10 shows the dependence of the temporal evolution of titanium ion density profiles on the transport parameters. Apart from the absolute value of each ionized charge state ion, the presence of a convective inward velocity ($C_V = 1$) brings no remarkable difference in the shape of profiles of total ion density and Ti^{20+} ion density, which takes the main part of the soft X-ray signals. Therefore, it would be very difficult to distinguish the difference in impurity transport from spatial profile of impurity ions due to the spectroscopic measurements. Impurity tracer experiment will become more important, because a slight difference in impurity transport appears in the time evolution. Impurity study using a tracer like as laser blow-off injection experiment has been carried out by utilizing a change of impurity level at an instantaneous limiter discharge during a divertor one. A more detailed transport analysis of those measurements will be reported later.

Acknowledgement

The authors wish to thank the members of JT-60 team who have contributed to the JT-60 project throughout its progress. Especially, we wish to express our appreciation to Dr. T. Fukuda for the submilimeter measurement, to Dr. M. Sato for the ECE measurement, to Dr. H. Yoshida for the Thomson scattering

measurement and to Drs. T. Nishitani and K. Nagashima for the soft X-ray measurement. Special thanks are due to Drs. Y. Shimomura and M. Azumi for fruitful discussions. The continuing support of Drs. S. Mori, K. Tomabechi, M. Yoshikawa and T. Iijima, is gratefully acknowledged.

References

1) FONCK, R., HULSE, R., Phys. Rev. Lett. 13 (1984) 530.

2) HIRAYAMA, T., TAKIZUKA, T., SHIMADA, M., NAGAMI, M., KONOSHIMA, S., et al., J. Nucl. Mate. 128&129 (1984) 271.

3) SHIMADA, M., WASHIZU, M., SENGOKU, S., SUZUKI, N., NAGAMI, M., et al., J. Nucl. Mate. 128&129 (1984) 340.

4) KEILHACKER, M., FUSSMANN, G., VON GIERKE, G., JANESCHITZ, G., KORNHERR, M., et al., in Plasma Physics and Controlled Nuclear Fusion Research 1984 (Proc. 10th Int. Conf. London, 1984), Vol.1, IAEA, Vienna (1985) 71.

5) IDA, K., FONCK, R., SESNIC, S., HULSE, R., LEBLANC, B., Observation of neoclassical-like impurity transport in the $q<1$ region of the PBX tokamak, Plasma Physics Laboratory, Report PPPL-2313 (1986).

6) TFR group, Nucl. Fusion 25 (1985) 1767.

7) BEHRINGER, K., CARLOAN, P., DENNE, B., DECKER, G., ENGELHARDT, W., et al., Nucl. Fusion 26 (1986) 751.

8) KOIDE, Y., YAMADA, K., YOSHIDA, H., NAKAMURA, H., NIIKURA, S., TSUJI, S., Radiation loss and global energy balance of ohmically heated divertor discharge in JT-60 tokamak, Japan Atomic Energy Research Institute, Report JAERI-M 86-056 (1986).

9) TANI, K., et al., Experimental Transport Analysis System in JT-60, to be published.

10) HIRAYAMA, T., et al., Library system for a one dimensional tokamak transport code, Japan Atomic Energy Research Institute Report, JAERI-M 82-204 (1982) (in Japanese).

11) KEILHACKER, M., LACKNER, K., BEHRINGER, K., et al., Physica Scripta, T2/2, (1982) 443.

12) HULSE, R. A., Nucl. Tech./Fusion, 3 (1983) 259. T2/2, (1982) 443.

13) KISHIMOTO, H., JT-60 Team, 7th Conf. on Plasma-Surface Interaction in Cont. Fus. Devices, (Princeton, 1986), to be published.

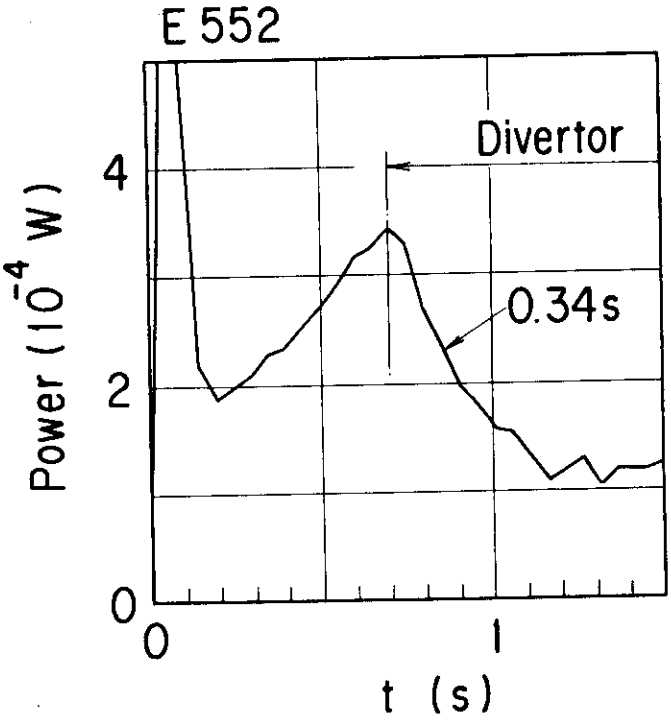

Fig. 1 The decay of impurity radiation power for the bolometric measurement, by changing a discharge mode from limiter to divertor.

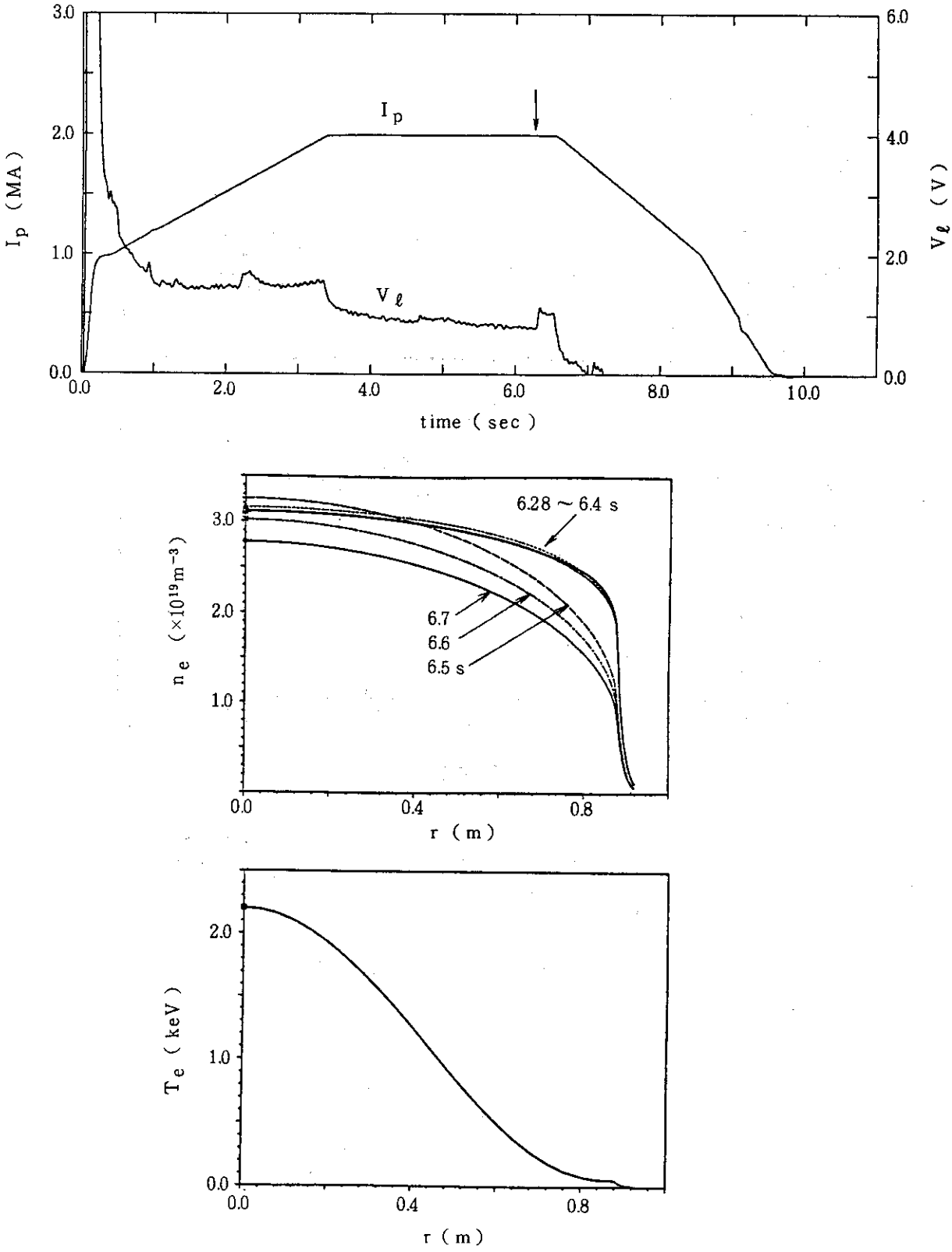

Fig. 2 The behaviour of plasma current and loop voltage for the shot of E1605 (top). The arrow shows the accidental titanium injection time. The temporal evolution of the electron density profile (middle) after the injection. The electron temperature profile applied to the calculation (bottom).

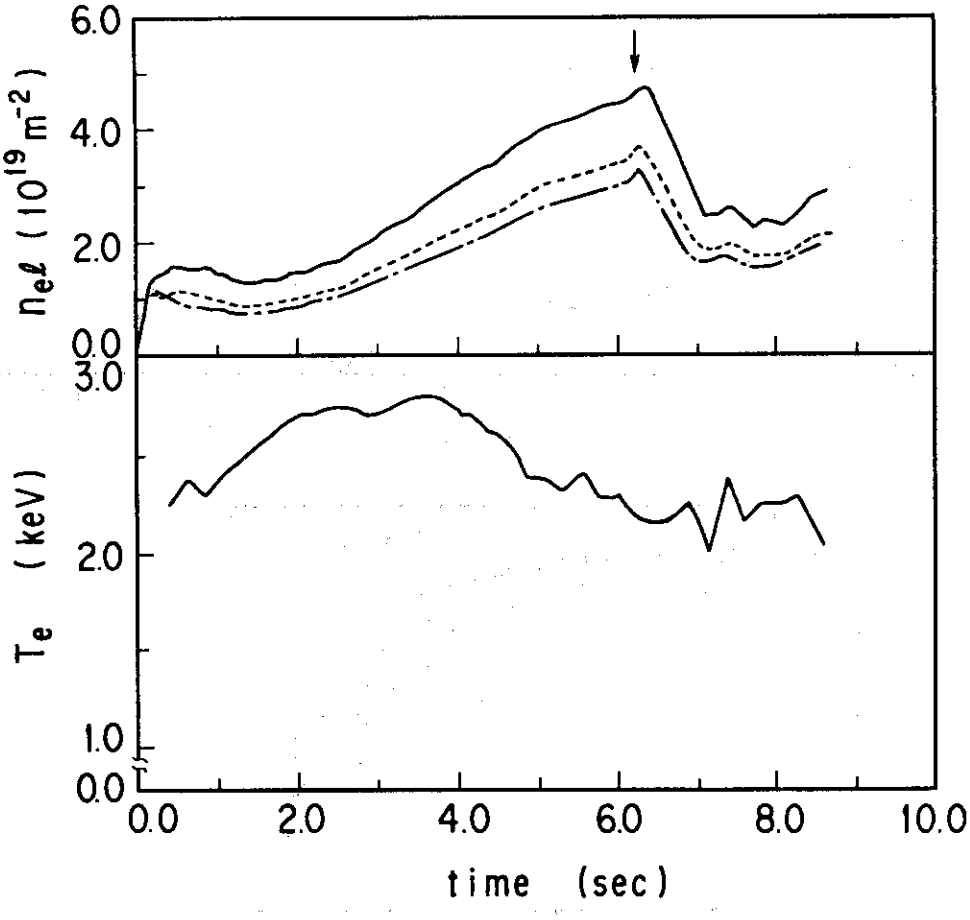

Fig. 3 The time evolution of chordal electron densities from the interferometers and the central electron temperature from ECE measurement. The arrow shows the accidental titanium injection time.

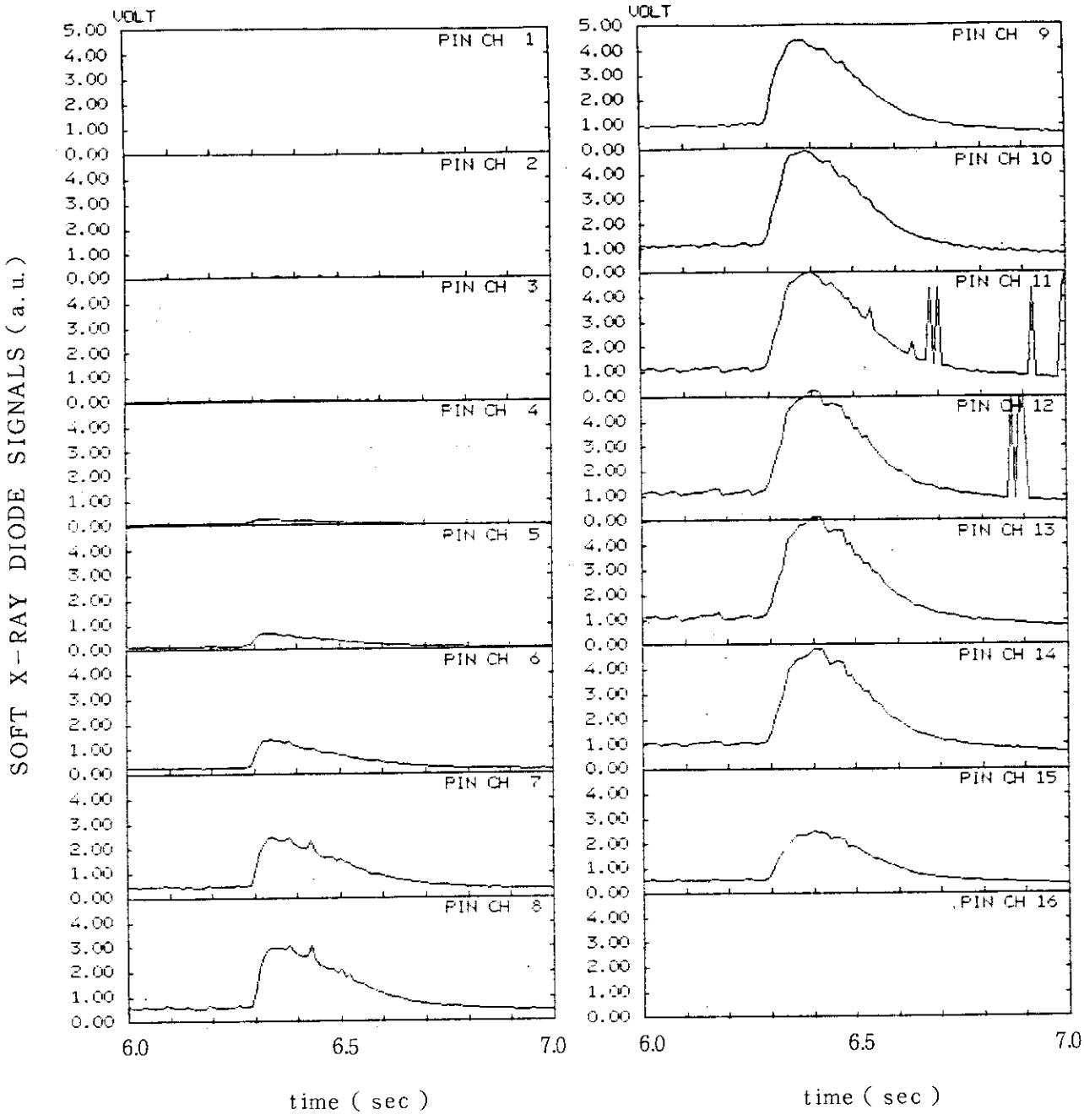

Fig. 4 The time evolutions of soft X-ray diode array signals for the shot of E1605. The channel numbers of 12 and 13 correspond to the radius position of ∿3.5 cm and ∿-3.5 cm from the plasma center. The distance between the channels is roughly 7 cm on the plasma center chord.

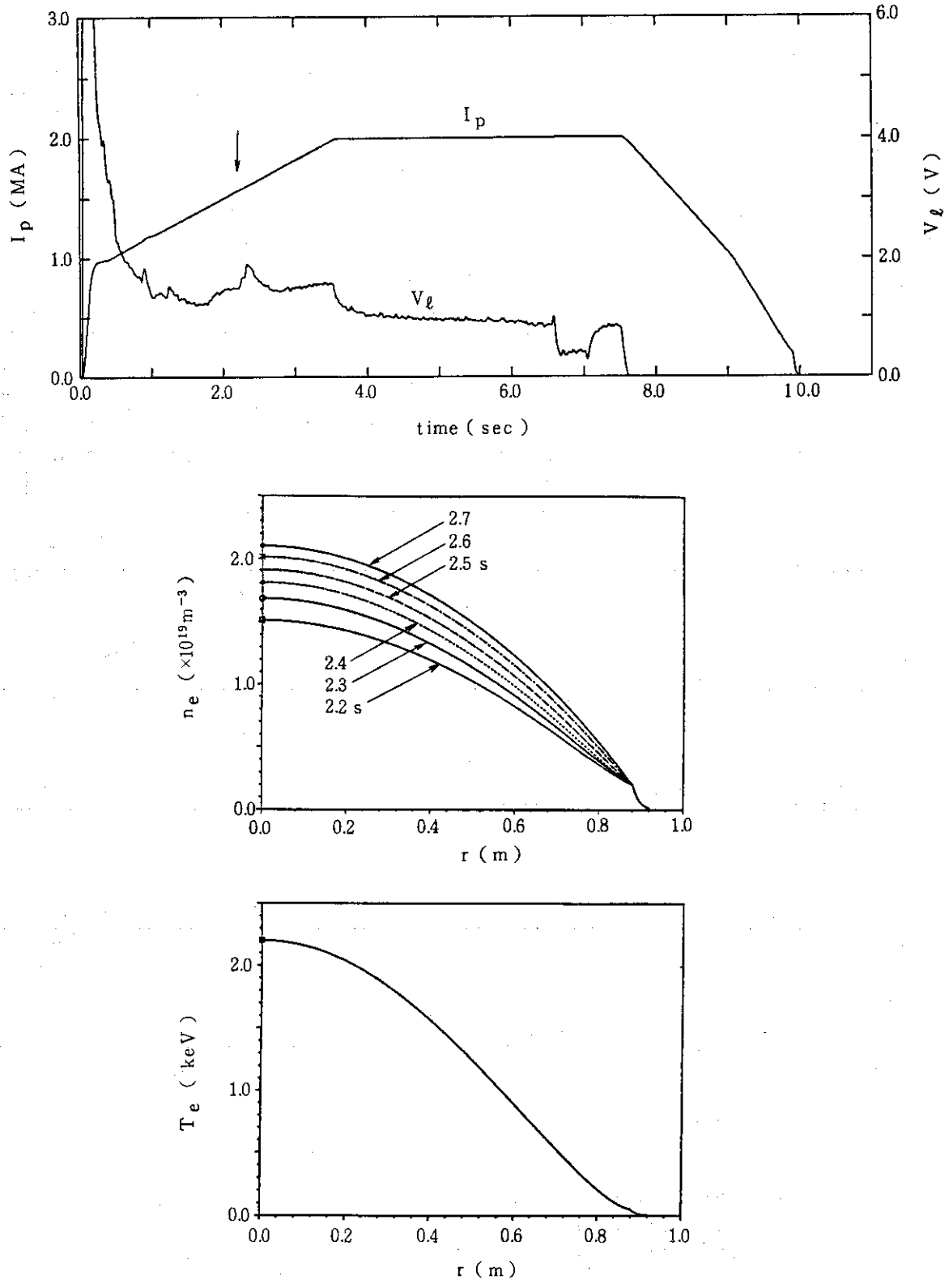

Fig. 5 The behaviour of plasma current and loop voltage for the shot of E1968 (top). The arrow shows the accidental titanium injection time. The temporal evolution of the electron density profile (middle) after the injection. The electron temperature profile applied to the calculation (bottom).

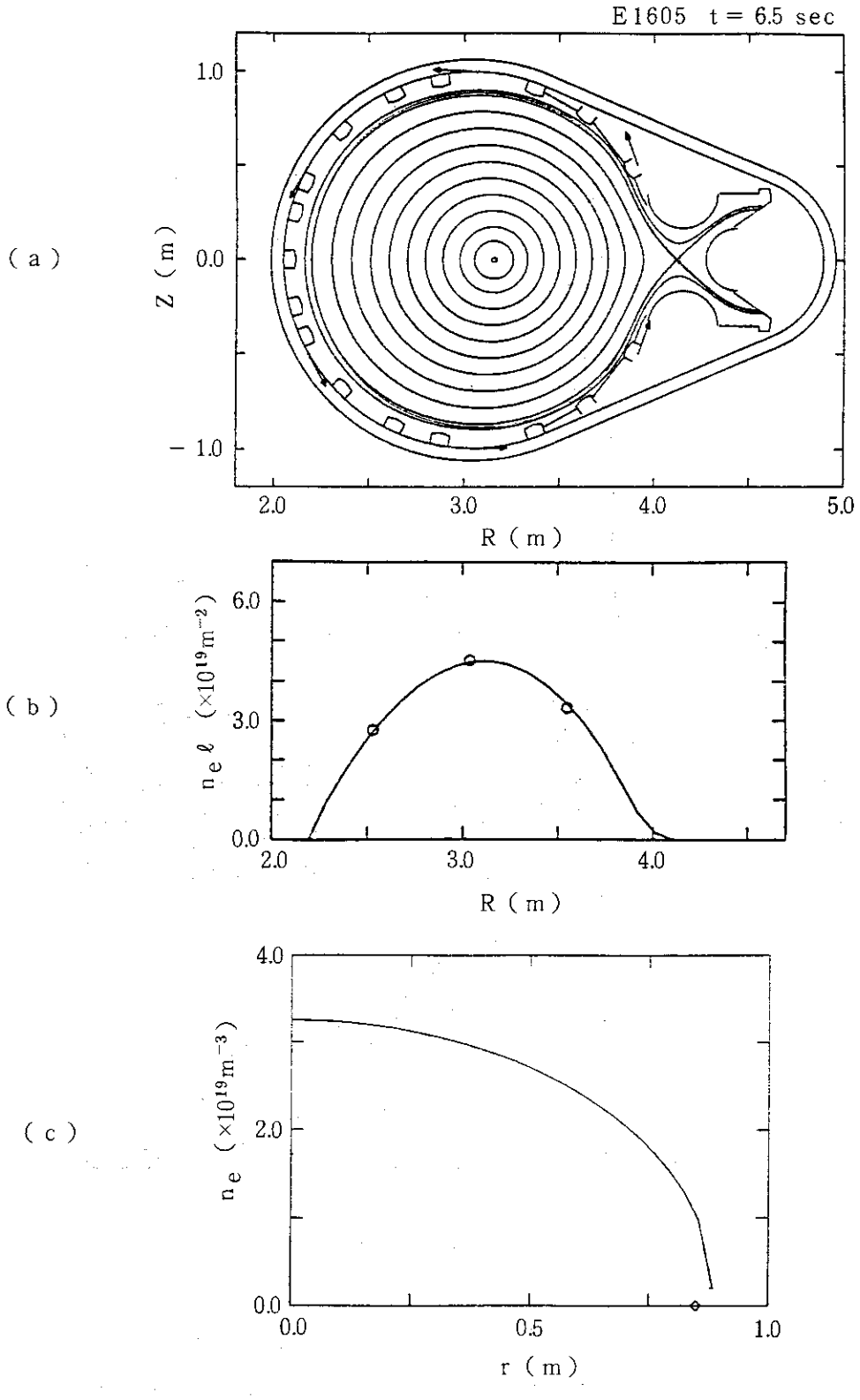

Fig. 6 a); magnetic flux surfaces estimated from the magnetic equilibrium code, at 6.5 sec for the shot of E1065 with plasma current I_p=2*MA*, b); the chordally integrated profile of fitted function shown as solid line and the values of three channel interferometer measurement shown as open circles, c); the electron density profile estimated from the fitted function, which is reduced to one-dimensional profile.

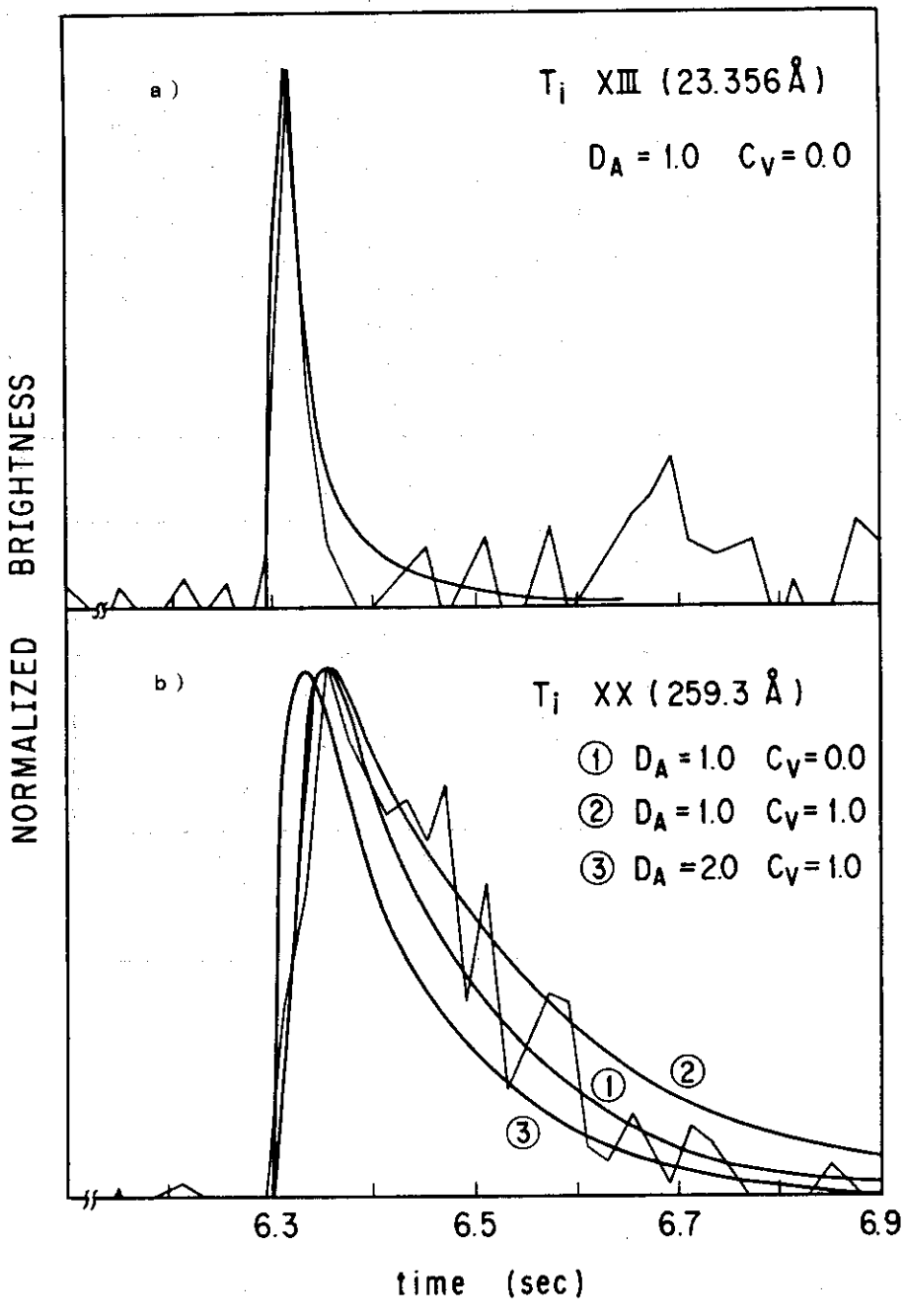

Fig. 7 a); the time evolution of experimental peripheral line radiance (T_i *XIII* 23.256 Å), which is subtracted the background level, and the simulated line radiance with $D_A = 1.0$ m^2/s and $C_V = 0.0$, b); the time evolution of experimental line radiance (T_i *XX* 259.3 Å), which is subtracted the background level, and the simulated line radiances,

1) D_A = 1.0 m^2/s, C_V = 0.0,
2) D_A = 1.0 m^2/s, C_V = 1.0,
3) D_A = 2.0 m^2/s, C_V = 1.0.

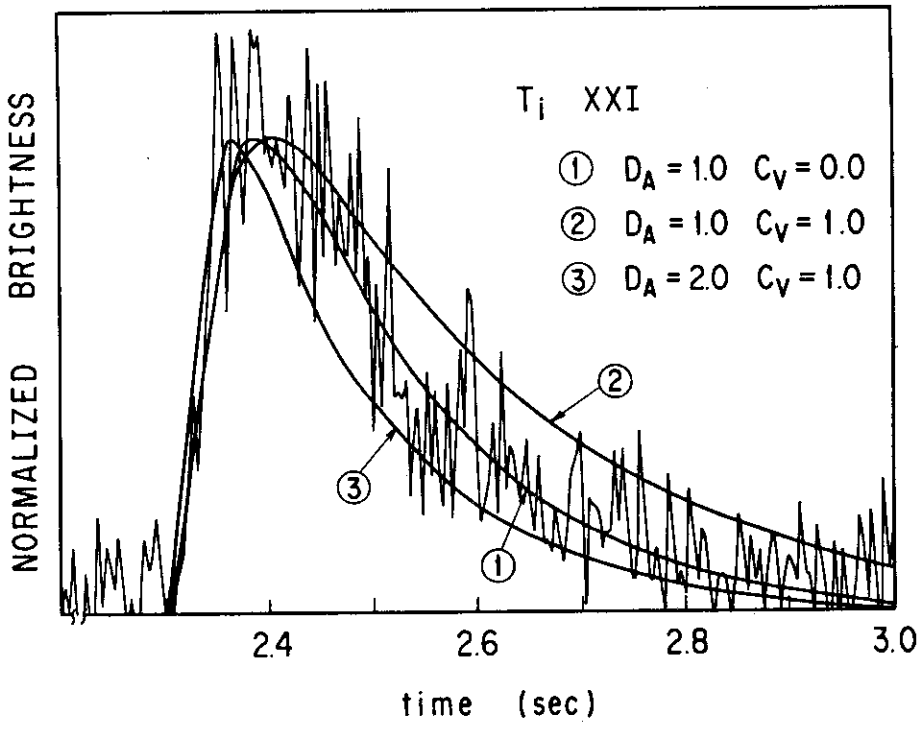

Fig. 8 The time evolution of the line radiance of center ion (T_i *XXI* resonance line), which is subtracted the background level, for the shot of E1968. The simulated lines are shown as the case with,

1) D_A = 1.0 m^2/s, C_V = 0.0,
2) D_A = 1.0 m^2/s, C_V = 1.0,
3) D_A = 2.0 m^2/s, C_V = 1.0.

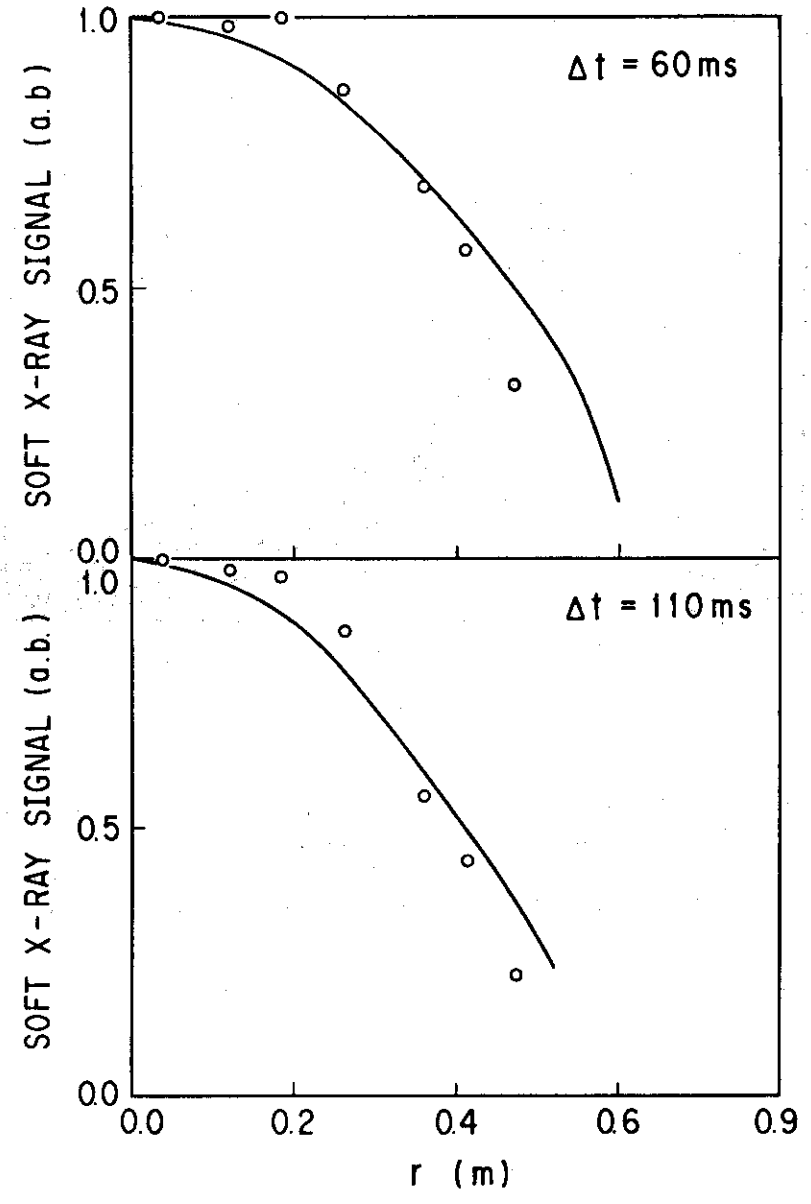

Fig. 9 The profile of soft X-ray signals form the fifteen channel diode arrays (open circles) for the shot of E1605 and from the calculation with D_A = 1.0 m^2/s and C_V = 0.0. The Δt shows the time after the accidental titanium injection at 6.3 sec.

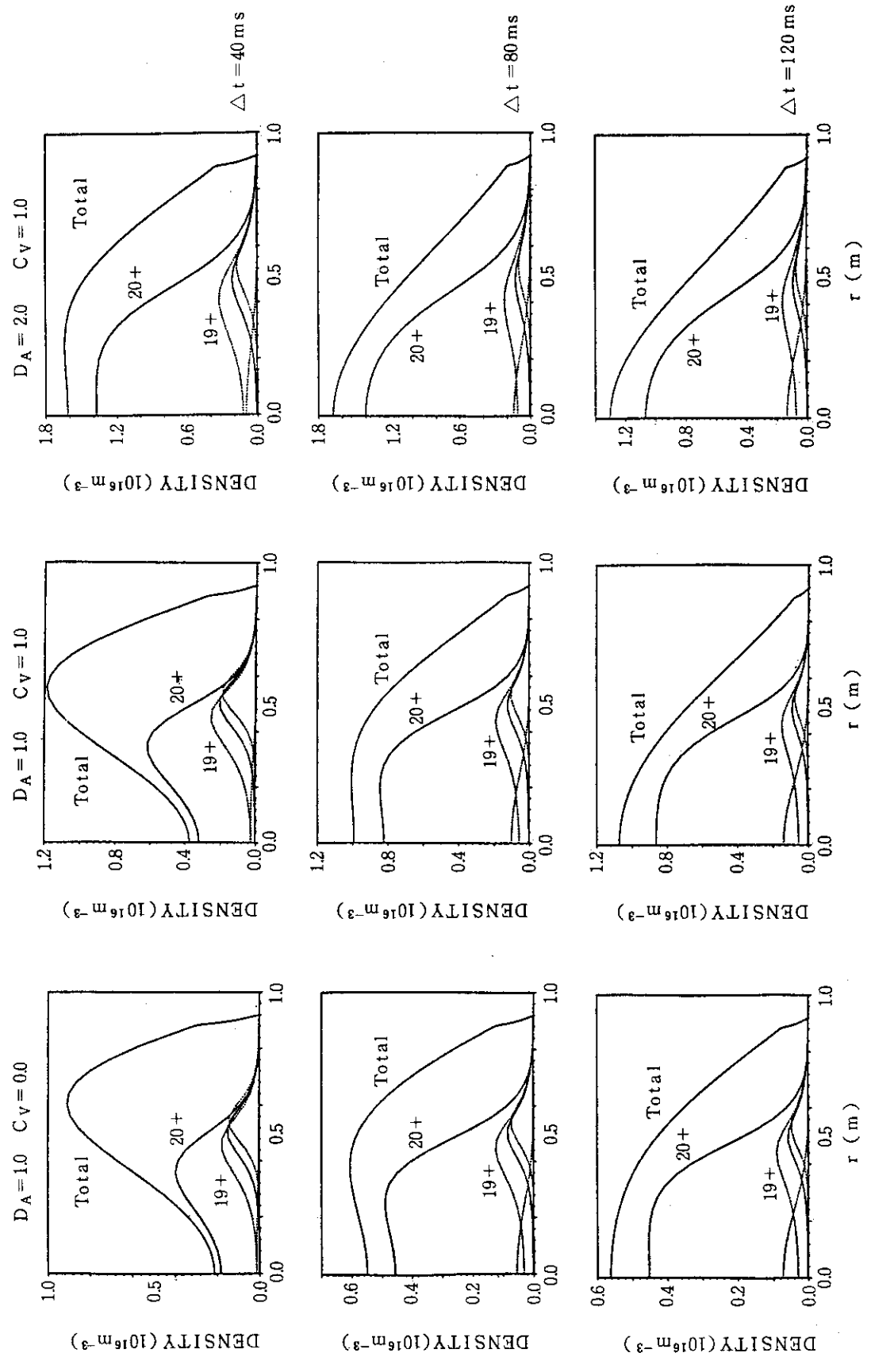

Fig. 10 The profiles of titanium ion density depending on the impurity transport parameters,

a) D_A = 1.0 m^2/s, C_V = 0.0,
b) D_A = 1.0 m^2/s, C_V = 1.0,
c) D_A = 2.0 m^2/s, C_V = 1.0.

The Δt shows the time after the accidental titanium injection at 6.3 sec.